BMC Psychiatry

RESEARCH

Open Access

Abnormal nonlinear features of EEG microstate sequence in obsessive–compulsive disorder

Huicong Ren[1†], Xiangying Ran[2,3,4,5†], Mengyue Qiu[2,3,4,5], Shiyang Lv[2,3,4,5], Junming Wang[2,3,4,5], Chang Wang[2,3,4,5], Yongtao Xu[2,3,4,5], Zhixian Gao[2,3,4,5], Wu Ren[2,3,4,5], Xuezhi Zhou[2,3,4,5], Junlin Mu[1], Yi Yu[2,3,4,5*] and Zongya Zhao[1,2,3,4,5,6*]

Abstract

Background At present, only a few studies have explored electroencephalography (EEG) microstates of patients with obsessive–compulsive disorder (OCD) and the results are inconsistent. Additionally, the nonlinear features of EEG microstate sequences contain rich information about the brain, yet how the nonlinear features of EEG microstate sequences abnormally change in patients with OCD is still unknown.

Methods Resting-state EEG data were collected from 48 OCD patients and macheted 48 healthy controls (HC). Subsequently, EEG microstate analysis was used to extract the microstate temporal parameters (duration, occurrence, coverage) and nonlinear features of EEG microstate sequences (sample entropy, Lempel–Ziv complexity, Hurst index). Finally, the temporal parameters and nonlinear features of EEG microstate sequences were sent to three kinds of machine learning models to classify OCD patients.

Results Both groups obtained four typical EEG microstate topographies. The duration of microstates A, B, and C in OCD patients decreased significantly, while the occurrence of microstate D increased significantly compared to HC. Sample entropy and Lempel–Ziv complexity of microstate sequences in OCD patients increased significantly, while Hurst index decreased significantly compared to HC. The classification accuracy using the nonlinear features of microstate sequences reached up to 85%, significantly higher than that based on microstate temporal parameter models.

Conclusion This study provides supplementary findings on EEG microstates in OCD patients with a larger sample size. We found that the nonlinear features of EEG microstate sequences in OCD patients can serve as potential electrophysiological biomarkers for distinguishing OCD patients.

Keywords Obsessive–compulsive disorder, EEG microstate, Nonlinear features, Machine learning

†Huicong Ren and Xiangying Ran contributed equally to this work and should be considered co-first authors.

*Correspondence:
Yi Yu
121012@xxmu.edu.cn
Zongya Zhao
zhaozongya_paper@126.com
Full list of author information is available at the end of the article

Introduction

Obsessive–compulsive disorder (OCD) is a serious mental disorder which affects a significant portion of the global population, with estimated prevalence rates ranging from 1 to 3% in each country [7]. While OCD can impact individuals of any age, it typically manifests in adolescence or early adulthood, characterized by recurrent obsessive thoughts and compulsive behaviors. This condition often induces extreme anxiety and distress, leading individuals to engage in a series of compulsive actions in an attempt to alleviate such feelings. These behaviors significantly impair patients' lives, affecting social and occupational functioning, and potentially leading to other mental health issues [15]. Therefore, research into and discovery of biomarkers for OCD have crucial clinical significance in early diagnosis.

Currently, non-invasive imaging techniques such as electroencephalography (EEG), magnetic resonance imaging (MRI) and functional near-infrared spectroscopy (fNIRS) have been employed in the auxiliary diagnosis and treatment of psychiatric and neurological disorders. Among them, EEG is widely used due to its advantages of low cost, no radiation, high temporal resolution, and suitability for long-term monitoring [31]. Numerous algorithms for extracting meaningful information from EEG signals have been proposed by scholars. Among the various analysis methods of EEG, microstate analysis is a relatively novel and popular algorithm. Microstate refers to a time window of brain electrical activity, typically lasting between 60–120 ms. In microstate analysis, EEG data is segmented into multiple microstates, each of which is believed to represent a specific functional state or information processing process in the brain, potentially serving as the basis for human cognitive functions [21, 32].

Numerous studies have shown that patients with psychiatric and neurological disorders exhibit abnormal changes in EEG microstate, such as schizophrenia [12], bipolar disorder [[43]], depression [46], and Parkinson's disease (PD) [10]. However, research of the microstates for OCD remains limited. To the best of our knowledge, only two studies have explored EEG microstate in OCD. Yoshimura et al.[45] found that, compared to the control group, OCD patients exhibited significantly higher occurrence of microstates A, B, and C during rest. Thirioux et al. [39] investigated the EEG microstates of OCD patients using high-density EEG, and found a significantly increased coverage of microstate C and shortened duration of microstate D in OCD patients. In conclusion, the results of the two studies were not consistent. This could be due to the small sample size of OCD patients included and the different number of microstate clusters, which affected the reliability and consistency of the OCD microstate results [38]. Therefore, further exploration of microstate research is needed in OCD patients.

In addition to microstate temporal parameters, microstate sequences also contain rich information about the brain. In recent years, some researchers have combined the nonlinear indicators with EEG microstate sequences to study the abnormal dynamics of brain networks in patients with psychiatric and neurological disorders. Our team previously investigated the sample entropy and Lempel–Ziv complexity (LZC) of EEG microstate sequences in first-episode drug-naive adolescents with depression and found that the sample entropy and LZC of depression patients were significantly higher than those of the healthy control group. In addition, these nonlinear features were used as features to classify patients with depression from healthy individuals based on machine learning method and achieved a high accuracy of 90.9% Zhao et al. [46, 47]. Murphy et al., [24] studied for the first time the sample entropy of EEG microstate sequence of schizophrenic patients, and the results showed that the sample entropy of schizophrenic patients increased significantly compared with healthy control group. Lassi et al. [20] used the LZC and Hurst exponent of EEG microstate sequences to distinguish patients with subjective cognitive decline (SCD), patients with mild cognitive impairment (MCI) and healthy controls. The results showed that the LZC of SCD patients was significantly higher than that of MCI patients, and the Hurst value of SCD and MCI patients was significantly lower than that of healthy people. It is suggested that the nonlinear features of EEG microstate sequence may be used as biomarkers to identify the progression to Alzheimer's Disease (AD) from its preclinical state. These research findings collectively suggest that the combination of microstate sequence with nonlinear features can reveal brain abnormalities in patients from a new perspective. However, there is limited research on the nonlinear features of OCD microstate sequences, and it remains unclear whether they exhibit abnormal changes. Therefore, we hypothesize that the nonlinear features of the EEG microstate sequence in OCD patients was abnormal, significantly increased sample entropy and LZC complexity in OCD patients and significantly lower Hurst index compared to HC.

In summary, there is limited research on EEG microstates in OCD, and the findings are inconsistent. Additionally, the nonlinear features of EEG microstate sequences in OCD have not been explored. Therefore, the aims of our research are: 1) to demonstrate the abnormality of nonlinear features of EEG microstate sequence in OCD patients and clarify whether they can serve as potential biomarkers for distinguishing OCD patients; 2) Considering the inconsistent findings between

Yoshimura et al. [45] and Thirioux et al. [39], provide a supplemental study about microstates of OCD patients with a larger sample size.

Materials and methods

Participants

The participants in this study consist of two parts. For the dataset 1, 57 OCD patients and 34 healthy controls (HC) were downloaded from a public database [42]. After EEG preprocessing, subjects with poor EEG signal quality were excluded, and 32 patients and 33 healthy subjects were retained. For dataset 2, 19 OCD patients and matched 17 healthy controls (HC) were recruited from the Second Affiliated Hospital of Xinxiang Medical University. After EEG preprocessing, subjects with poor EEG signal quality were excluded, and 16 patients and 15 HC were retained. In summary, a total of 48 OCD patients and 48 healthy controls were included in this study for subsequent EEG microstate analysis, and Table 1 shows the demographic information. Independent sample T-test showed no significant difference between OCD and HC in gender ($P=0.362$) and age ($P=0.475$).

All OCD patients underwent detailed behavioral and neuropsychiatric evaluations, and subjects were excluded if they were at significant risk of suicide, had a history of neurological disease, seizures, serious somatic illness, or had a history of drug or alcohol dependence or personality disorders. All enrolled patients were obsessive–compulsive disorder patients with a Yale-Browne score (Y-BOCS) of 16 or greater. For dataset 2, the study followed the Declaration of Helsinki was and approved by the Ethics Committee of the Second Affiliated Hospital of Xinxiang Medical University with the written informed consent of all participants.

EEG data acquisition

For dataset 1, 26-channel EEG recordings (FP1, FP2, F7, F3, Fz, F4, F8, FC3, FCz, FC4, T3, C3, Cz, C4, T4, CP3, CPz, CP4, P7/T5, P3, Pz, P4, P8/T6, O1, Oz, O2) based on the 10–10 international system using a Compumedics Quickcap were acquired at a sampling rate of 500 Hz.

Table 1 Demographic information

		Age(years) Mean ± std	Sex Male/Female	Y-BOCS
OCD	dataset1	30.74 ± 9.52	19/13	26.44 ± 8.89
	dataset2	27.88 ± 10.67	10/6	28.32 ± 6.50
	merge	29.78 ± 9.90	29/19	27.46 ± 6.36
HC	dataset1	32.17 ± 15.67	10/23	—
	dataset2	20.27 ± 1.79	11/4	—
	merge	27.47 ± 6.13	21/27	—

EEG data were collected for two minutes of open eye (EO) and two minutes of closed eye (EC), and participants were asked to remain relaxed during the recording. But only EEG data from EC was used for subsequent processing analysis. The impedance of recording electrodes was kept less than 10 KΩ. For dataset 2, 64-channel resting-state EEG signals based on the 10–20 International system (Neuroscan SynAmps2, Australia). EEG data were recorded from each subject who was asked to sit comfortably in a chair with their eyes closed for about 10 min. The EEG sampling frequency was set to 1000 Hz, and the electrode impedance was also kept below 10 kΩ.

EEG data preprocessing

Offline EEG data preprocessing was carried out using MATLAB 2013b software (The MathWorks Inc. Natick, MA, USA) equipped with EEGLAB toolbox [13]. We extracted 19 channels (Fp1, Fp2, F7, F3, Fz, F4, F8, T3, C3, Cz, C4, T4, T5, P3, Pz, P4, T6, O1, O2) from dataset 1 and dataset 2 at the same locations. The next preprocessing operations for dataset 1 and dataset 2 remained consistent. Firstly, a zero-phase FIR bandpass filter was applied to the EEG data in the 2–20 Hz range. Secondly, the EEG data were downsampled to 250 Hz. Thirdly, independent component analysis (ICA) was employed to identify and remove artifacts such as electrooculography (EOG), electromyography (EMG), electrocardiography (ECG), and poor channels [22]. Among them, 2.08 ± 1.40 (mean ± sd) components were deleted from HC and 2.44 ± 1.61 (mean ± sd) components from OCD. Fourthly, the data were segmented into 2-s intervals, with segments containing significant artifacts removed. The clear data segments were then concatenated. Finally, the first 90 s (epochs) of EEG data from each participant were selected for microstate analysis.

Microstates analysis

A microstate analysis toolbox was used to perform microstates analysis for resting-state EEG data [27]. As shown in Fig. 1, the process of EEG microstate analysis was briefly described as follows. Firstly, we calculated the global field power (GFP) for each participant at each time point

$$GFP = \sqrt{\frac{\sum_{i=1}^{n} u_i^2}{n}} \quad (1)$$

Here, i represents each electrode, u denotes the measured EEG potential of each channel, and n represents the number of electrodes (here is 19). Based on the above equation, we could obtain an GFP curve that reflects the degree of change in the EEG potential between all electrodes in a given time. Because the local maximum of

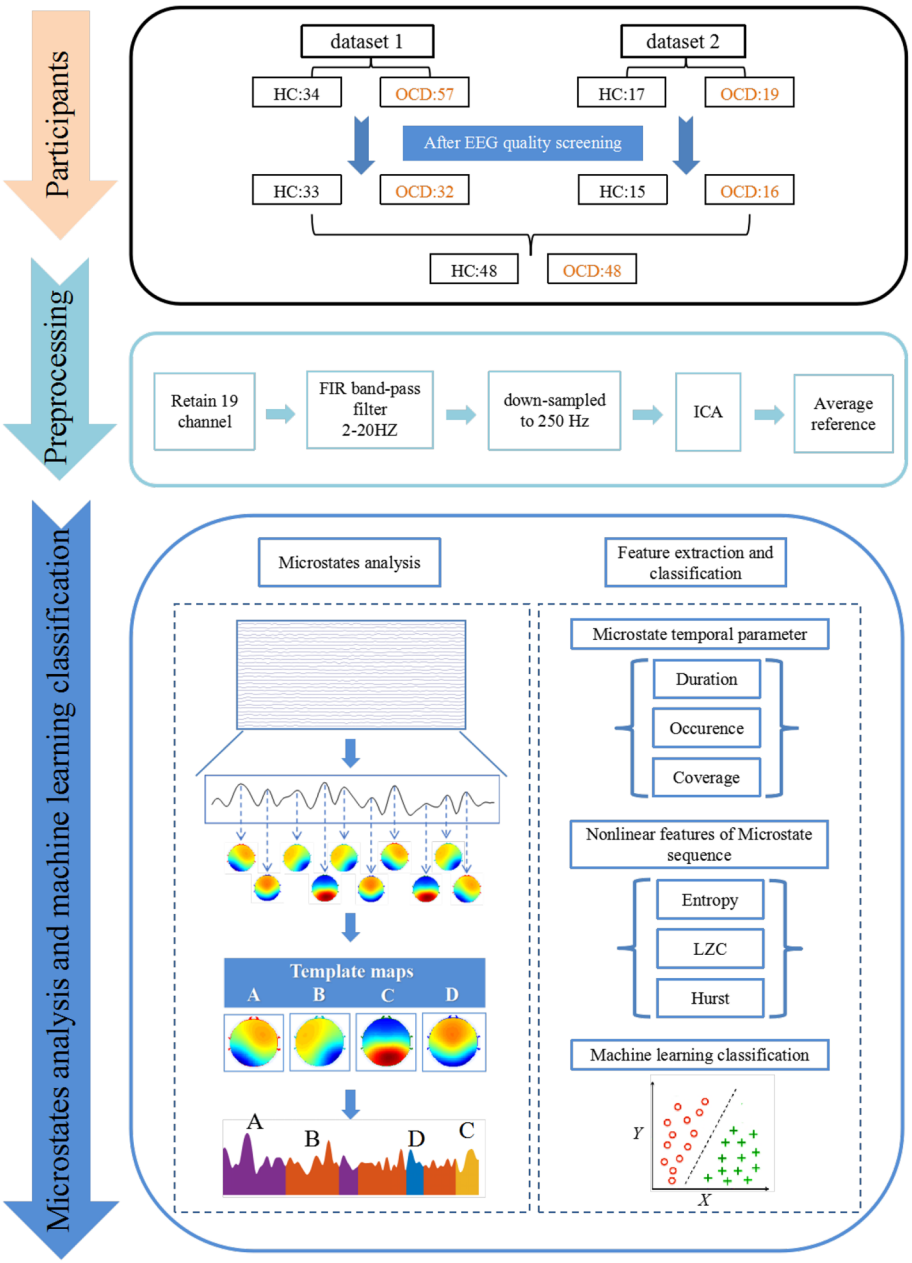

Fig. 1 Flow chart of materials and methods. The processes of participants screening, EEG preprocessing, microstate analysis, feature extraction and classification are summarized. (HC: healthy controls; OCD: obsessive–compulsive disorder; ICA: independent component analysis; LZC: Lempel–Ziv complexity)

the GFP curve has the strongest signal intensity and the highest signal-to-noise ratio, therefore, the topographic maps at the GFP local maximum point (called original maps) were selected for subsequent clustering analysis.

Firstly, an improved k-means algorithm was employed for clustering, with the number of clusters set between 2 and 8. Secondly, Cross-Validation criterion(CV) was used to determine the optimal number of clusters, which was found to be 4 for both the OCD and HC groups. Thirdly, the program randomly selects four types of brain topographic maps as the initial clustering centers, compares and updates other topographic maps with the initial clustering centers based on spatial correlation, and recalculates the global interpretation variance GEV until the highest and stable GEV appears. At this time, the four clustering centers obtained are microstate "template

maps":A、B、C、D. Finally, spatial correlation was used to map the four "template maps" back to EEG data, with each time point labeled according to the microstate category with the highest correlation. After the above microstate analysis, the related EEG microstate temporal features for each subject were extracted:

(a) Duration: the average length of time for each microstate (unit: ms).
(b) Occurrence: the average number of occurrences per second for each microstate (unit: Hz).
(c) Coverage: time coverage percentage of each microstate across total analysis time (unit: %).

Entropy calculation

Sample entropy calculates the likelihood of creating a new pattern in the signal, which allows it to quantify time series and complexity. The sequence complexity increases with the likelihood of producing a new pattern [23]. In this study, sample entropy was used to characterize the complexity of the microstate sequence for each individual. The detailed algorithm of sample entropy was described in Zhao et al., [47]. Briefly, computation of samp entropy depends on two key parameters: a template length m and a tolerance r. In this study, we labeled the microstates with the numbers 1–4(For example, ABCD → 1234), r is set to 0.1 and m ranged from 1 to 10 [24]. In order to eliminate the influence of the different m, the average sample entropy was computed with m ranging from 1 to 10.

LZC calculation

LZC is a complexity measurement method which quantifies the randomness and unpredictability of a sequence by analyzing the pattern repeatability in the sequence. The original Lempel–Ziv complexity algorithm consists of transformation of the signal into a binary sequence by comparing it with the threshold (e.g., mean or median) and calculating the unique subsequence in a sequence [4]. The lower the LZC value, the more repeated patterns in the sequence which indicates the lower complexity. On the contrary, the higher the LZC value, the higher the randomness and complexity of the sequence. In this study, we apply the improved LZC algorithm for microstate sequences [37, 47]. The EEG microstate sequence consists of a string of A, B, C, and D, which we simplify into a transition sequence. For example, if the original sequence is AAAABBBCCCDAADD, the transition sequence would be ABCDAD, containing only the state transitions. Given that the lengths of the transition sequences vary among participants after conversion, it is necessary to choose a sufficiently small number N to ensure that all participants' transition sequences are greater than or equal to this value. In this study, we chose $N = 1200$.

Hurst index

Hurst index is an indicator used to quantify the long-term memory properties of time series, which evaluates the long-term dependence of the time series based on the asymptotic behavior of the autocorrelation function. The Hurst index ranges between 0 and 1, where $H = 0.5$ indicates that the sequence is random and has no long-term memory; $H > 0.5$ indicates that the sequence has a positive long-term dependence, and $H < 0.5$ indicates that the sequence has a negative long-term dependence [20]. In this study, we used the DFA (Detrended Fluctuation Analysis) toolbox in MATLAB to compute the Hurst exponent. During the calculation, we configured multiple time scales ranging from 50 to 500 data points, with a step size of 50, to ensure robust and reliable results.

Machine learning classification

To evaluate whether microstate temporal parameters (duration, occurrence, coverage) or nonlinear features of microstate sequences (entropy, LZC, and Hurst) could serve as potential biomarkers for distinguishing OCD patients, both feature sets were sent to machine learning models for classification. Firstly, we extracted three temporal parameters (duration, occurrence, and coverage) for each of the four microstates (A, B, C, D), resulting in 12 temporal parameters, which formed feature set 1 (Set 1). Next, we extracted three nonlinear features of the microstate sequences—entropy, LZC, and the Hurst—as feature set 2 (Set 2). Subsequently, both feature sets were sent to three machine learning models (Support Vector Machine (SVM) [47], Logistic Regression (LR) [2], and Gaussian Naive Bayes (GNB) [28] for classification of OCD patients from HC. Finally, multiple metrics based on fivefold cross-validation, including accuracy (ACC), sensitivity (SEN), specificity (SPE), and area under the receiver operating characteristic (ROC) curve (AUC), were used to comprehensively evaluate the classification performance of the models. All classification steps were performed using Python version 2.8.2 with default parameters, equipped with scikit-learn library version 0.24.2.

Statistical analysis

We employed the Ragu toolbox for Topographic Analysis of Variance(TANOVA) to investigate whether there are statistical differences in microstate topographies A, B, C, and D between OCD and HC. SPSS 19.0 software was used for the statistical analysis, and data were represented as mean ± standard deviation(std). The Shapiro–Wilk test was employed to determine whether the

distribution was normal. Each microstate measure was compared of between OCD patients and healthy subjects using Wilcoxon rank sum test if the data does not conform to a normal distribution and false discovery rate (FDR) correction was used to control multiple comparison problem. We used Cohen's d as a measure of the effect size of the pairwise comparisons. Finally, Pearson correlation analysis was used to explore whether there was a significant correlation between the time parameters of microstate, the nonlinear features of microstate sequences and Y-BOCS scores.

Result

EEG microstate temporal parameters

As shown in Fig. 2, four typical EEG microstate topographic maps were obtained for OCD patients and healthy controls which are consistent with the findings of most previous studies [17, 18, 48]. In order to assess the explanatory power of the microstate topographic maps for the EEG data, the global explained variance (GEV) between the two groups was compared. The results showed that the GEV was 0.7464 ± 0.0423 (mean ± std) for the HC group and 0.7264 ± 0.0547 (mean ± std) for the OCD group, and Wilcoxon rank sum test indicated no statistical difference in GEV between the two groups ($P = 0.0912$, z value = 1.6890). However, the TANOVA revealed a significant difference in microstate D topography between OCD and HC ($P = 0.027$).

In order to quantitatively explore the differences between the OCD and HC groups, we extracted the temporal parameters of each microstate including duration, occurrence and coverage. It is found that only LZC ($P = 0.3595, W = 0.974$) and Entropy ($P = 0.0998, W = 0.9599$) conform to normal distribution in HC. In OCD, only the occurrence of microstate D ($P = 0.2280, W = 0.970$) and Hurst index ($P = 0.8540, W = 0.9866$) conform to normal distribution. Therefore, we used Wilcoxon rank sum test to conduct differential statistics. We found that the average duration of microstates A, B, and C in the OCD group was significantly lower than those of HC group (Fig. 3A and Table 2). In terms of occurrence, the average occurrence frequency of microstate D in the OCD group was significantly higher than that in the HC group (Fig. 3B and Table 2). However, there was no significant difference in the average coverage (Fig. 3C and Table 2).

Nonlinear features of EEG microstate sequence

The EEG microstate sequence contains rich information of the whole brain. We employed three nonlinear features including sample entropy, LZC, and Hurst index to quantify the nonlinear features of EEG microstate sequences in the OCD and HC groups. We found that the sample entropy of the OCD group was significantly higher than that of the HC group (Fig. 4A and Table 2; $P_{fdr} = 0.0069$). Similarly, the average LZC of the OCD group was also significantly higher than that of the HC group (Fig. 4B and Table 2; $P_{fdr} = 0.0007$), indicating a greater unpredictability and chaos in the brain state of OCD patients. However, the Hurst index of the OCD group was significantly lower than that of the HC group and its value was relatively closer to 0.5 (Fig. 4C and Table 2; Pfdr = 0.0001), which may indicate weaker long-term memory and stability in their brain network activity.

We used Pearson correlation analysis to explore whether there was a correlation between the time parameters of microstate, the nonlinear features of microstate sequences and the severity of obsessive–compulsive disorder (Y-BOCS scores), and none of them showed significant correlations.

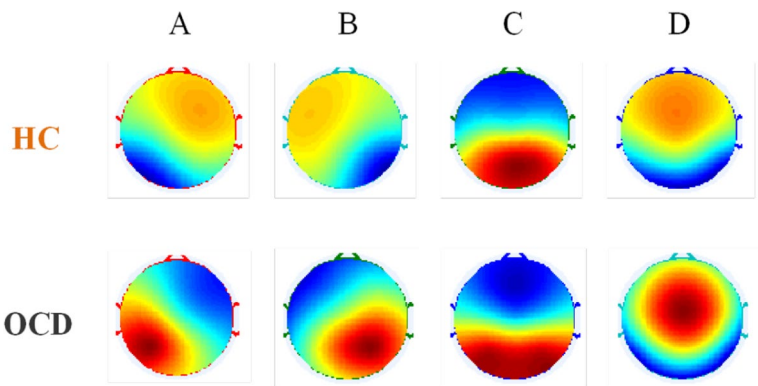

Fig. 2 Topographic maps of four types of EEG microstates (microstates A-D) in HC and OCD group. (HC:healthy controls; OCD: obsessive–compulsive disorder)

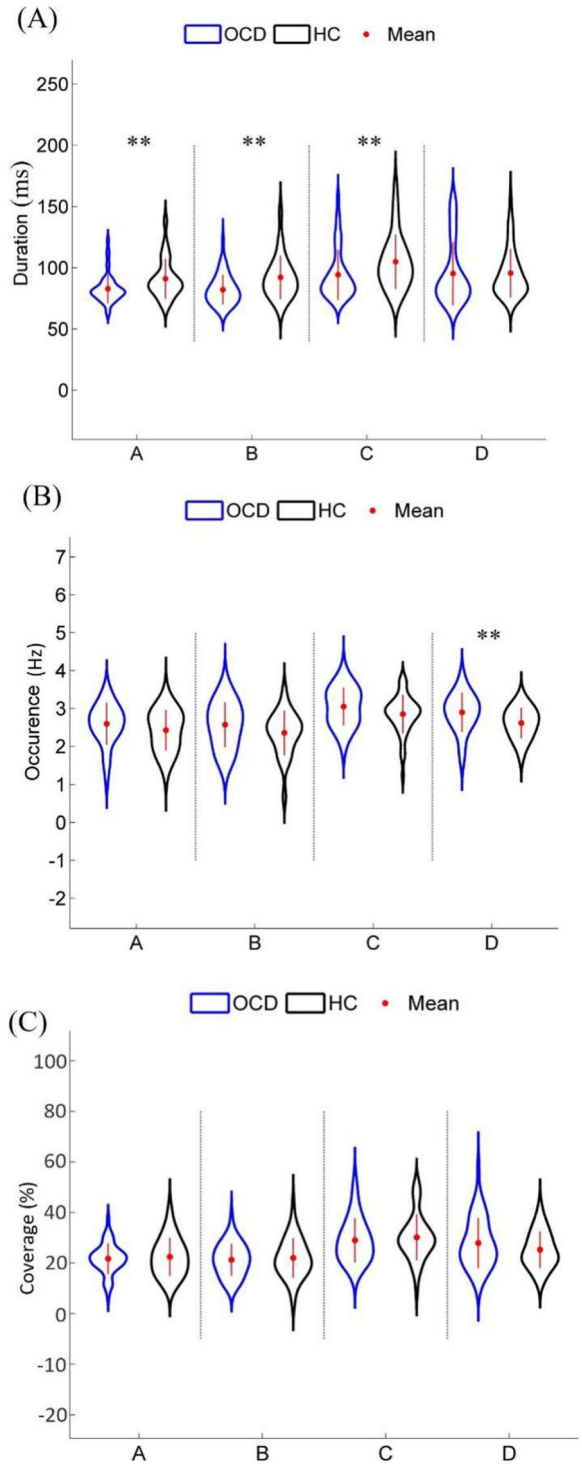

Fig. 3 Comparison of the EEG microstate temporal parameters between OCD and HC groups: **A** Duration, **B** Occurrence, and **C** Coverage. '**' indicates $P_{fdr} < 0.01$. (HC:healthy controls; OCD:obsessive–compulsive disorder)

Machine learning classification

The above results indicate that there exist statistical differences between OCD and HC for microstate temporal parameters and nonlinear features of microstate sequence. However, it is unclear whether these microstate temporal parameters or nonlinear features of microstate sequence can serve as potential biomarkers for OCD based on machine learning method. Here, two types of feature sets were sent to SVM, LR, and GNB machine learning models for classification of OCD between HC: 1) microstate temporal parameters (Set 1) and 2) nonlinear features of microstate sequence (Set 2). As shown in Table 3 and Fig. 5, as for feature set 1, the classification accuracies of SVM, LR, and GNB models are 75.86%, 72.41%, and 75.86%, respectively. For feature set 2, the classification accuracies of the three machine learning models are 80%, 85%, and 80%, respectively, significantly higher than those based on feature set 1. The results indicate that the nonlinear features of EEG microstate sequences can effectively and stably enhance the classification performance, demonstrating that the nonlinear features of EEG microstate sequences can serve as potential biomarkers for distinguishing OCD.

Discussion

In this study, we combined EEG microstate temporal parameters and nonlinear features of microstate sequence to reveal the abnormal brain network dynamics of OCD patients. We found that both OCD and HC obtained four typical EEG microstate topographies. For the microstate temporal parameters, the average duration of microstates A, B, and C in OCD was significantly lower than that in HC, while the average occurrence of microstate D in OCD was significantly higher than that in HC. As for microstate sequence nonlinear features, the average Entropy and LZC values in OCD were significantly higher than those in HC, while the average Hurst value was significantly lower in OCD than in HC. Finally, using microstate temporal parameters and microstate sequence nonlinear features as feature sets for classifying OCD and HC, we found that the classification accuracy based on the latter was significantly higher than that based on the former.

The abnormal microstate temporal parameters in OCD

Previous studies have indicated that microstate A reflects the auditory network (AN), primarily associated with the bilateral temporal cortex [6]. Cottraux et al. [11] found that compared to healthy controls, adult OCD patients exhibited higher cerebral blood flow trends in the temporal region, suggesting abnormal auditory information processing in the temporal

Table 2 Comparison of EEG microstate temporal parameters and nonlinear features of microstate sequence between OCD and HC group

	HC		OCD					
	Mean	**std**	**Mean**	**std**	**P**	***Z* value**	**Cohen's d**	P_{fdr}
Duration								
Class A	91.0865	16.2325	82.9108	11.6718	0.0028	-2.9860	-0.5783	**0.0048**
Class B	92.2596	17.6140	82.1848	12.1643	0.0015	-3.1839	-0.6656	**0.0048**
Class C	104.9997	22.1774	94.3411	20.4936	0.0036	-2.9127	-0.4992	**0.0048**
Class D	95.6367	19.8856	95.2714	25.8056	0.3243	-0.9856	-	0.3243
Occurrence								
Class A	2.4287	0.5342	2.5968	0.5488	0.1311	1.5096	-	0.1311
Class B	2.3572	0.5860	2.5722	0.5919	0.1007	1.6415	-	0.1311
Class C	2.8516	0.5095	3.0509	0.4988	0.1151	1.5756	-	0.1311
Class D	2.6178	0.4012	2.9002	0.5142	0.0017	3.1401	0.6122	**0.0068**
Coverage								
Class A	22.47	7.54	21.73	6.03	0.8633	-0.1722	-	0.8633
Class B	22.05	7.75	21.30	6.30	0.6628	-0.4360	-	0.8633
Class C	30.21	9.09	29.02	8.72	0.3694	-0.8976	-	0.7388
Class D	25.27	7.19	27.95	9.85	0.2576	1.1321	-	0.7388
Entropy	0.0891	0.0153	0.0986	0.0195	0.0069	-2.7002	-0.5424	**0.0069**
LZC	470.2083	45.1027	502.521	48.9233	0.0005	-3.4736	-0.6867	**0.0008**
Hurst	0.6914	0.0551	0.6436	0.0490	< 0.0001	4.1071	0.9178	**0.0001**

HC healthy controls, *OCD* obsessive–compulsive disorder, *std* standard deviation

lobe of OCD patients. Korostenskaja et al. [19] found similar auditory information processing abnormalities in adolescent OCD patients. Microstate B reflects the visual network (VN), primarily involving the bilateral occipital cortex [1]. Pujol et al. [29] found that cortical intralayer functional connectivity in the visual cortex was weaker in OCD patients than in healthy individuals. Chapman et al. [8] found abnormalities in early visual processing in OCD patients. Other studies also have found changes in the brain structure of OCD patients in the occipital and parietal lobes [35, 36, 40, 41]. Microstate C reflects the default mode network (DMN), associated with the bilateral insula, bilateral inferior frontal cortex, and anterior cingulate cortex, while microstate D reflects the dorsal attention network (DAN) and executive control network (ECN), involving the medial prefrontal cortex, cingulate gyrus, and posterior parietal cortex [5, 25]. Studies based on functional magnetic resonance imaging (fMRI) technology ave shown abnormalities in the DMN, ECN, and their associated brain regions in OCD patients. Fan et al., [14] found significant abnormal interactions between the salience network (SN), DMN, and ECN in OCD patients. Similarly, Sha et al. [33] used resting-state fMRI technology to discover abnormally increased functional connectivity between the left caudate nucleus and dorsolateral prefrontal cortex in OCD patients. The aforementioned studies indirectly support our findings that the duration of microstates A, B, and C in OCD was significantly lower than that in HC, while the average occurrence of microstate D in OCD was significantly higher than that in HC. Our findings are supported by the study of Cheng et al. [9], who found a significantly shorter duration of microstate A and significantly increased occurrence of microstate D in OCD compared to HC. However, our findings are inconsistent with the results of the two previous studies on EEG microstates in OCD patients. In the study by Yoshimura et al. [45], OCD patients showed significantly higher occurrence rates of microstates A, B, and C during rest compared to the healthy controls. In the study by Thirioux et al. [39], OCD patients showed a significant increase in the coverage of microstate C compared to healthy individuals, while the duration of microstate D was significantly reduced. This discrepancy may be attributed to the limited sample size of OCD patients included or inconsistencies in the number of EEG microstate obtained in the previous studies. In addition, the heterogeneity of OCD patients and the impact of therapeutic drugs may also lead to these inconsistent results. In conclusion, this study provides a supplemental result about the microstates of OCD patients with a larger sample size.

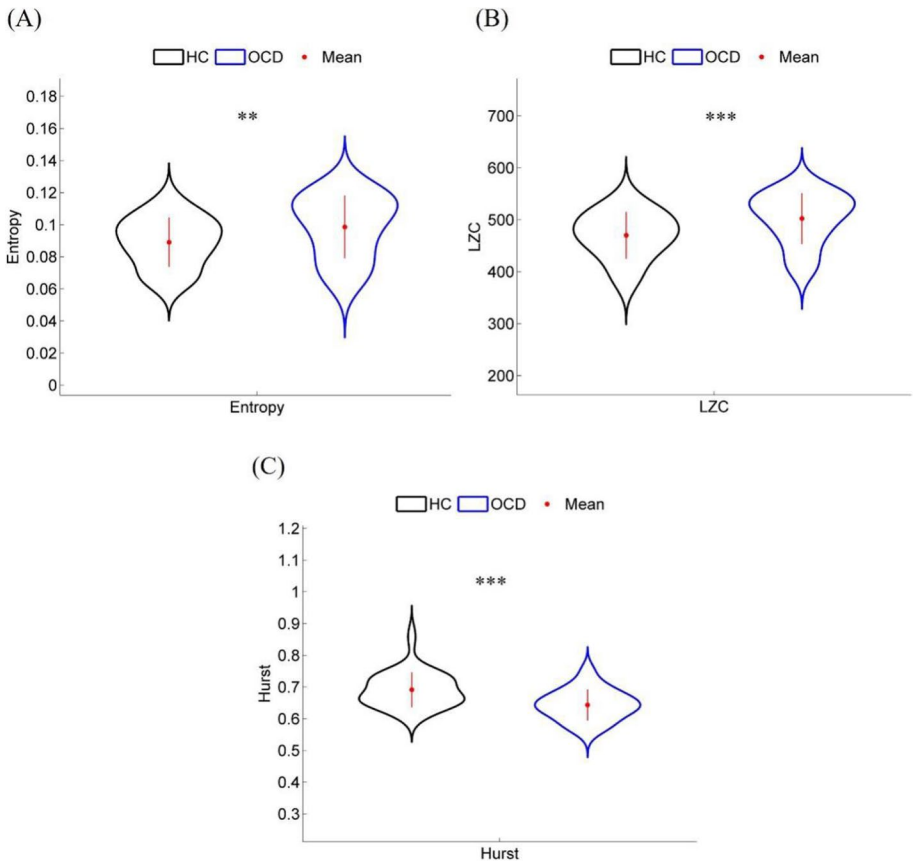

Fig. 4 Nonlinear features of EEG microstate sequence in OCD and HC groups: **A** Entropy, **B** LZC and **C** Hurst. '**' and '***' indicate $P_{fdr} < 0.01$ and $P_{fdr} < 0.001$, respectively. (HC: healthy controls; OCD: obsessive–compulsive disorder)

Table 3 Classification performance based on feature Set 1 and Set 2 for three kinds of machine learning models

Methods	ACC	SEN	SPE	AUC
Set 1				
SVM	75.86%	76.47%	75.0%	77.0%
LR	72.41%	70.59%	75.0%	71.0%
GNB	75.86%	82.35%	66.67%	77.0%
Set 2				
SVM	80.0%	83.0%	68.0%	90.0%
LR	85.0%	93.0%	84.0%	94.0%
GNB	80.0%	90.0%	73.0%	92.0%

SVM support vector machine, *LR* logistic regression, *GNB* gaussian naive bayes, *ACC* accuracy, *SEN* sensitivity, *SPE* specificity, *AUC* area under the receiver operating characteristic curve

The nonlinear features of EEG microstate sequence used as potential neurophysiological biomarkers of OCD

Sample entropy is a metric quantifying the complexity of time series, capable of measuring irregularity and predictive uncertainty within data [23]. LZC is a complexity measure grounded in information theory, utilized to assess the quantity of new and repeated patterns within time series data [4]. Thus, the increase in values of sample entropy and LZC can indicate the randomness and complexity of data. Sample entropy and LZC are increasingly widely applied in psychiatric and neurological disorders to assess the complexity of EEG microstate sequences such as Alzheimer's disease [20], depression [47], and psychosis [24]. Currently, there exists no research applying sample entropy and LZC to study the EEG microstate sequences of OCD. In this study, we utilized sample entropy and LZC to assess the irregularity and complexity of EEG microstate sequences in OCD patients. Our findings revealed that OCD patients exhibit higher levels of sample entropy and LZC compared to healthy controls. Jiang et al. [16] computed brain entropy for OCD and HC groups based on resting-state fMRI, and found that OCD patients showed significantly increased approximate entropy and fuzzy entropy across nearly the entire brain compared to the control group. Blair et al. [3] projected dynamic functional connectivity of resting-state fMRI into a low-dimensional space

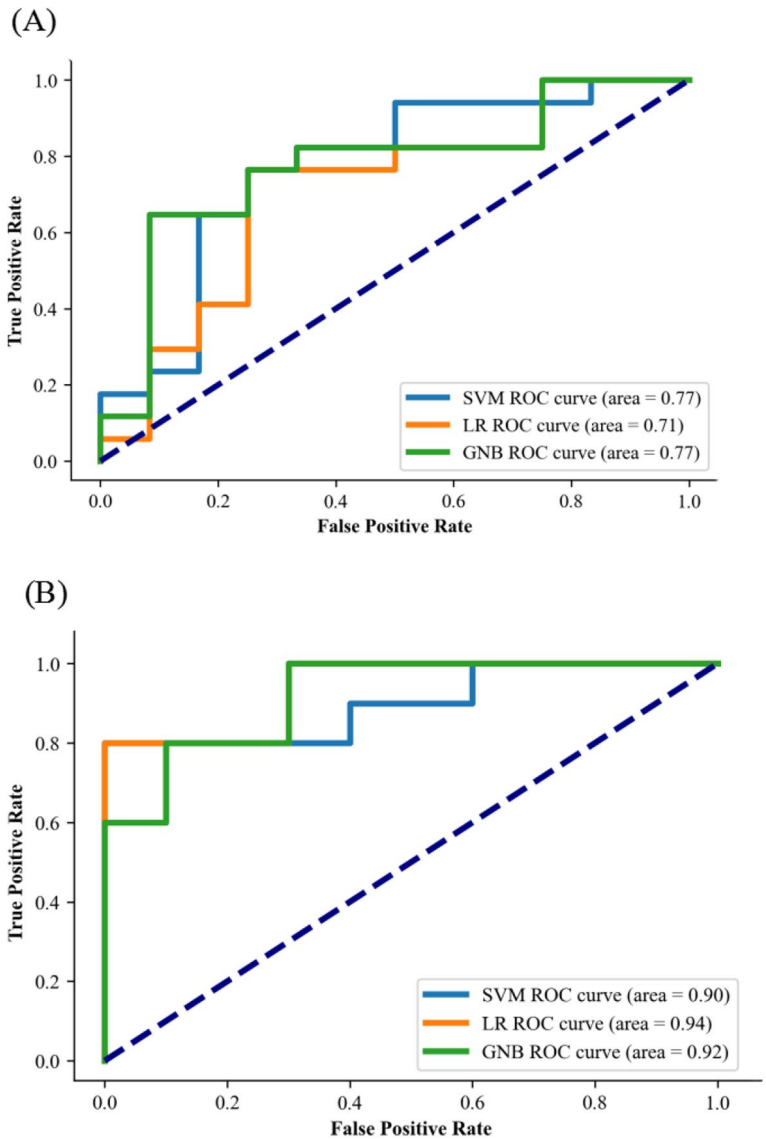

Fig. 5 ROC curve of (**A**) three machine learning classification using microstate temporal parameters (duration, occurrence and coverage) and (**B**) three machine learning classification based on nonlinear features of microstate sequence (entropy, LZC and Hurst). (SVM: support vector machine; LR: logistic regression; GNB: gaussian naive bayes; ROC: receiver operating characteristic)

and dimension-specific entropy was estimated within this space, similarly finding higher entropy values in OCD patients compared to healthy controls. These findings are consistent with our results, indicating that OCD patients exhibit higher randomness, unpredictability and complexity in their brain network. The increased random complexity in OCD patients may be related to cognitive control and executive function deficits in individuals with OCD. During task execution, individuals with OCD may need to mobilize more cognitive resources to process information due to cognitive deficits, which may lead to increased complexity in brain activity [34]. Moreover, the typical symptoms of OCD, such as the cyclical nature of obsessive thoughts and the repetitiveness of behaviors [15], may also be reflected as increased complexity in brain activity.

The Hurst index is a metric used to measure the long-term memory of time series data. In healthy individuals, higher Hurst values are typically associated with better cognitive function and stronger neural stability [49]. Observed Hurst values in OCD patients significantly decrease and approach 0.5, indicating weaker long-term memory and stability in their brain network activity. This finding may be related to the reduced cognitive flexibility

observed in OCD patients [30]. This aligns with the pathological features of OCD patients struggling to break free from obsessive thoughts and behaviors [15]. In summary, changes in sample entropy, LZC, and Hurst values in OCD patients may reveal the neural basis of their cognitive control and executive function impairments.

The above results showed that there exist significantly statistical differences in EEG microstate temporal parameters and nonlinear measures of microstate sequence between healthy controls and OCD patients, in this study, we further combined machine learning method and microstate features to classify OCD patients at individual level for the first time. Our results showed that a good classification performance (accuracy = 85.0%) was obtained when nonlinear measures of EEG microstate sequence was sent to LR machine learning model. Our classification performance was apparently better than those of some previous literature based on machine learning classification of OCD patients. For example, Yang et al. [44] extracted fractional amplitude low-frequency fluctuation (fALFF) of resting-state fMRI, and applied support vector machine (SVM) to distinguish between OCD patients and healthy controls, achieving an accuracy of 72%. Park et al. [26] extracted gamma-band functional connectivity from EEG signals, and used elastic net machine classification method to classify OCD patients, achieving an accuracy of 74.52%. In conclusion, our results demonstrate that these nonlinear measures of EEG microstate sequence can be used as a potential biomarker for the auxiliary classification of OCD patients.

Limitations and future directions

However, this study still has some limitations that need to be considered. Firstly, since the subjects included in the study originated from two different datasets, differences in data acquisition equipment may have some impact on the results. Secondly, although the sample size of OCD patients in this study is larger than previous studies, more studies are needed to confirm our findings in the future. Thirdly, OCD patients in dataset 2 are using drugs at the time when they received the experiment, while detailed information on the medication status of OCD patients is not provided in dataset 1, so more detailed recording and control of participants are needed in future studies. Finally, although we found that nonlinear features of EEG microstate sequence can serve as potential biomarkers of OCD patients, a follow-up study may be needed to track longitudinal changes in nonlinear features at different stages of OCD patients.

Authors' contributions

R.H. R.X. Q.M. L.S. and W.J. wrote the main manuscript. W.C. X.Y. G.Z. R.W. Z.X. M.J. Y.Y. and Z.Z. reviewed the manuscript.

Funding

This work was supported by the National Natural Science Foundation of China (No. 82201709 and 82302298), the Science and Technology Research Project of Henan Province (No. 242102310055, 232102310009, 242102310005, 242102521012), the Open Project Program of Henan Collaborative Innovation Center of Prevention and Treatment of Mental Disorder (No. XTkf07, XTkf01, XTgh02, XTgh01), the Open Project Program of the First Affiliated Hospital of Xinxiang Medical University (No.XZZX2022009), the Innovative Research Team (in Science and Technology) in University of Henan Province (No. 24IRTSTHN042), Major science and technology projects of Henan Province (No. 221100310500), the Open Program of Henan Key Laboratory of Biological Psychiatry (No. ZDSYS2022008), the Science and Technology Research Program Project of Xinxiang City (No. GG2021013), the Open Program of Henan Clinical Research Center for Mental Disorders (No. 2021-zxkfkt-007), and the Henan Province medical science and technology research plan joint construction project (No. LHGJ20230539).

Data availability

The data and materials that support the findings of this study are available from the corresponding author, [Zongya Zhao, zhaozongya_paper@126.com], upon reasonable request.

Declarations

Ethics approval and consent to participate

For the second part of participants, the study followed the Declaration of Helsinkiwas and approved by the Ethics Committee of the Second Affiliated Hospital of Xinxiang Medical University with the written informed consent of all participants.

Consent for publication

All subjects agreed to participate in the study.

Competing interests

The authors declare no competing interests.

Author details

[1]Henan Collaborative Innovation Center of Prevention and Treatment of Mental Disorder, The Second Affiliated Hospital of Xinxiang Medical University, Xinxiang, People's Republic of China. [2]School of Medical Engineering, School of Mathematical Medicine, Xinxiang Medical University, Xinxiang, People's Republic of China. [3]Engineering Technology Research Center of Neurosense and Control of Henan Province, Xinxiang, People's Republic of China. [4]Henan International Joint Laboratory of Neural Information Analysis and Drug Intelligent Design, Xinxiang, People's Republic of China. [5]Henan Engineering Research Center of Medical VR Intelligent Sensing Feedback, Xinxiang, People's Republic of China. [6]The First Affiliated Hospital of Xinxiang Medical University, Weihui, People's Republic of China.

Received: 23 June 2024 Accepted: 22 November 2024
Published online: 04 December 2024

References

1. Al Zoubi O, Mayeli A, Misaki M, et al. Canonical EEG microstates transitions reflect switching among BOLD resting state networks and predict fMRI signal. J Neural Eng. 2022;18(6):https://doi.org/10.1088/1741-2552/ac4595.
2. Alotaibi S, Atta-ur-Rahman, Basheer MI, Khan MA. Ensemble machine learning based identification of pediatric epilepsy. Comput Mater Contin. 2021;68(1):149–65. https://doi.org/10.32604/cmc.2021.015976.
3. Blair DS, Soriano-Mas C, Cabral J, Moreira P, Morgado P, Deco G. Complexity changes in functional state dynamics suggest focal connectivity reductions. Front Hum Neurosci. 2022;16:958706.
4. Borowska M. Multiscale Permutation Lempel-Ziv Complexity Measure for Biomedical Signal Analysis: Interpretation and Application to Focal EEG Signals. Entropy (Basel). 2021;23(7):832.

5. Bréchet L, Brunet D, Birot G, Gruetter R, Michel CM, Jorge J. Capturing the spatiotemporal dynamics of self-generated, task-initiated thoughts with EEG and fMRI. Neuroimage. 2019;194:82–92.
6. Britz J, Van De Ville D, Michel CM. BOLD correlates of EEG topography reveal rapid resting-state network dynamics. Neuroimage. 2010;52(4):1162–70.
7. Chalah MA, Ayache SS. Could Transcranial Direct Current Stimulation Join the Therapeutic Armamentarium in Obsessive-Compulsive Disorder? Brain Sci. 2020;10(2):125.
8. Chapman EA, Martinez S, Keil A, Mathews CA. Early visual perceptual processing is altered in obsessive-compulsive disorder. Clin Neurophysiol. 2023;151:134–42.
9. Cheng J, Wang Y, Tang Y, Lin L, Gao J, Wang Z. EEG microstates are associated with the improvement of obsessive-compulsive symptoms after transcranial direct current stimulation. J Psychiatr Res. 2024;176:360–7.
10. Chu C, Wang X, Cai L, et al. Spatiotemporal EEG microstate analysis in drug-free patients with Parkinson's disease. Neuroimage Clin. 2020;25:102132.
11. Cottraux J, Gérard D, Cinotti L, et al. A controlled positron emission tomography study of obsessive and neutral auditory stimulation in obsessive-compulsive disorder with checking rituals. Psychiatry Res. 1996;60(2–3):101–12.
12. Cruz JR, Favrod O, Roinishvili M, et al. EEG microstates are a candidate endophenotype for schizophrenia. Nat Commun. 2020;11(1):3089. Published 2020 Jun 18.
13. Delorme A, Makeig S. EEGLAB: an open source toolbox for analysis of single-trial EEG dynamics including independent component analysis. J Neurosci Methods. 2004;134(1):9–21.
14. Fan J, Zhong M, Gan J, et al. Altered connectivity within and between the default mode, central executive, and salience networks in obsessive-compulsive disorder. J Affect Disord. 2017;223:106–14.
15. Gragnani A, Zaccari V, Femia G, et al. Cognitive-Behavioral Treatment of Obsessive-Compulsive Disorder: The Results of a Naturalistic Outcomes Study. J Clin Med. 2022;11(10):2762. Published 2022 May 13.
16. Jiang X, Li X, Xing H, Huang X, Xu X, Li J. Brain Entropy Study on Obsessive-Compulsive Disorder Using Resting-State fMRI. Front Psychiatry. 2021;12:764328.
17. Koenig T, Lehmann D, Merlo MC, Kochi K, Hell D, Koukkou M. A deviant EEG brain microstate in acute, neuroleptic-naive schizophrenics at rest. Eur Arch Psychiatry Clin Neurosci. 1999;249(4):205–11.
18. Koenig T, Prichep L, Lehmann D, Sosa PV, Braeker E, Kleinlogel H, Isenhart R, John ER. Millisecond by millisecond, year by year: normative EEG microstates and developmental stages. Neuroimage. 2002May;16(1):41–8.
19. Korostenskaja M, Harris E, Giovanetti C, et al. Magnetoencephalography reveals altered auditory information processing in youth with obsessive-compulsive disorder. Psychiatry Res. 2013;212(2):132–40.
20. Lassi M, Fabbiani C, Mazzeo S, et al. Degradation of EEG microstates patterns in subjective cognitive decline and mild cognitive impairment: Early biomarkers along the Alzheimer's Disease continuum? Neuroimage Clin. 2023;38:103407.
21. Lehmann D, Ozaki H, Pal I. EEG alpha map series: brain micro-states by space-oriented adaptive segmentation. Electroencephalogr Clin Neurophysiol. 1987;67(3):271–88.
22. Liang A, Zhao S, Song J, Zhang Y, Zhang Y, Niu X, Xiao T, Chi A. Treatment Effect of Exercise Intervention for Female College Students with Depression: Analysis of Electroencephalogram Microstates and Power Spectrum. Sustainability. 2021;13(12):6822.
23. Liu Q, Ma L, Fan SZ, Abbod MF, Shieh JS. Sample entropy analysis for the estimating depth of anaesthesia through human EEG signal at different levels of unconsciousness during surgeries. PeerJ. 2018;6:e4817.
24. Murphy M, Stickgold R, Öngür D. Electroencephalogram Microstate Abnormalities in Early-Course Psychosis. Biol Psychiatry Cogn Neurosci Neuroimaging. 2020;5(1):35–44.
25. Musso F, Brinkmeyer J, Mobascher A, Warbrick T, Winterer G. Spontaneous brain activity and EEG microstates. A novel EEG/fMRI analysis approach to explore resting-state networks. Neuroimage. 2010;52(4):1149–1161.
26. Park SM, Jeong B, Oh DY, et al. Identification of Major Psychiatric Disorders From Resting-State Electroencephalography Using a Machine Learning Approach. Front Psychiatry. 2021;12:707581.
27. Poulsen, A. T., Pedroni, A., Langer, N., and Hansen, L. K. Microstate EEGlab toolbox: an introductory guide. 2018, bioRxiv [Preprint].
28. Prastyo PH. Predicting breast cancer: A comparative analysis of machine learning algorithms. Proceeding international conference on science and technology. 2020. https://doi.org/10.14421/icse.v3.545.
29. Pujol J, Blanco-Hinojo L, Maciá D, et al. Mapping Alterations of the Functional Structure of the Cerebral Cortex in Obsessive-Compulsive Disorder. Cereb Cortex. 2019;29(11):4753–62.
30. Robbins TW. Cognitive flexibility, OCD and the brain. Brain. 2022;145(3):814–5.
31. Salahuddin U, Gao PX. Signal Generation, Acquisition, and Processing in Brain Machine Interfaces: A Unified Review. Front Neurosci. 2021;15:728178.
32. Schumacher J, Peraza LR, Firbank M, Thomas AJ, Kaiser M, Gallagher P, O'Brien JT, Blamire AM, Taylor JP. Dysfunctional brain dynamics and their origin in Lewy body dementia. Brain. 2019;142(6):1767–82.
33. Sha Z, Versace A, Edmiston EK, et al. Functional disruption in prefrontal-striatal network in obsessive-compulsive disorder. Psychiatry Res Neuroimaging. 2020;300:111081.
34. Silveira VP, Frydman I, Fontenelle LF, et al. Exploring response inhibition and error monitoring in obsessive-compulsive disorder. J Psychiatr Res. 2020;126:26–33.
35. Spalletta G, Piras F, Fagioli S, Caltagirone C, Piras F. Brain microstructural changes and cognitive correlates in patients with pure obsessive compulsive disorder. Brain Behav. 2014;4(2):261–77.
36. Szeszko PR, Christian C, Macmaster F, et al. Gray matter structural alterations in psychotropic drug-naive pediatric obsessive-compulsive disorder: an optimized voxel-based morphometry study. Am J Psychiatry. 2008;165(10):1299–307.
37. Tait L, Tamagnini F, Stothart G, et al. EEG microstate complexity for aiding early diagnosis of Alzheimer's disease. Sci Rep. 2020;10(1):17627.
38. Tarailis P, Koenig T, Michel CM, Griškova-Bulanova I. The Functional Aspects of Resting EEG Microstates: A Systematic Review. Brain Topogr. 2024;37(2):181–217.
39. Thirioux B, Langbour N, Bokam P, et al. Microstates imbalance is associated with a functional dysregulation of the resting-state networks in obsessive-compulsive disorder: a high-density electrical neuroimaging study using the TESS method. Cereb Cortex. 2023;33(6):2593–611.
40. Togao O, Yoshiura T, Nakao T, et al. Regional gray and white matter volume abnormalities in obsessive-compulsive disorder: a voxel-based morphometry study. Psychiatry Res. 2010;184(1):29–37.
41. Valente AA Jr, Miguel EC, Castro CC, et al. Regional gray matter abnormalities in obsessive-compulsive disorder: a voxel-based morphometry study. Biol Psychiatry. 2005;58(6):479–87.
42. van Dijk H, van Wingen G, Denys D, Olbrich S, van Ruth R, Arns M. The two decades brainclinics research archive for insights in neurophysiology (TDBRAIN) database. Sci Data. 2022;9(1):333.
43. Wang F, Hujjaree K, Wang X. Electroencephalographic Microstates in Schizophrenia and Bipolar Disorder. Front Psychiatry. 2021;12:638722.
44. Yang X, Hu X, Tang W, et al. Multivariate classification of drug-naive obsessive-compulsive disorder patients and healthy controls by applying an SVM to resting-state functional MRI data. BMC Psychiatry. 2019;19(1):210.
45. Yoshimura M, Pascual-Marqui RD, Nishida K, et al. Hyperactivation of the Frontal Control Network Revealed by Symptom Provocation in Obsessive-Compulsive Disorder Using EEG Microstate and sLORETA Analyses. Neuropsychobiology. 2019;77(4):176–85.
46. Zhao S, Ng SC, Khoo S, Chi A. Temporal and Spatial Dynamics of EEG Features in Female College Students with Subclinical Depression. Int J Environ Res Public Health. 2022(a);19(3):1778.
47. Zhao Z, Niu Y, Zhao X, et al. EEG microstate in first-episode drug-naive adolescents with depression. J Neural Eng. 2022(b);19(5). https://doi.org/10.1088/1741-2552/ac88f6.
48. Zhao Z, Ran X, Lv S, Wang J, Qiu M, Wang C, Xu Y, Guo X, Gao Z, Mu J, Yu Y. Causal link between prefrontal cortex and EEG microstates: evidence from patients with prefrontal lesion. Front Neurosci. 2023;14(17):1306120.
49. Zhuang C, Meidenbauer KL, Kardan O, et al. Scale invariance in fNIRS as a measurement of cognitive load. Cortex. 2022;154:62–76.

Publisher's Note